



Available online at www.sciencedirect.com


ScienceDirect
 Journal of Hydrodynamics
 2008,20(1):117-124



sdj.chinajournal.net.cn

INCIPIENT MOTION OF NON-COHESIVE SEDIMENT UNDER ICE COVER – AN EXPERIMENTAL STUDY*

WANG Jun

School of Civil Engineering, Hefei University of Technology, Hefei 230009, China,

E-mail: wangjunhfut@126.com

SUI Jue-yi

Environmental Science and Environmental Engineering Program, University of Northern British Columbia, British Columbia, Canada, V2N 4Z9

KARNEY Bryan W.

Department of Civil Engineering, University of Toronto, Toronto, Ontario, Canada, M5S 1A4

(Received September 3, 2007, Revised November 3, 2007)

Abstract: Based on a series of experiments under both ice-covered and free surface conditions, the present article discusses the role of flow velocity and critical shear Reynolds number for incipient motion of bed material. The influence of the resistance coefficients of both the underside of the ice cover and the channel bed on the location of the maximum velocity has been discussed. In addition, the impacts of ice and composite resistance coefficients on flow velocity for incipient motion of bed material have been assessed. The diagram describing the critical shear Reynolds number and the dimensionless shear stress for the incipient motion of sediment under ice covered conditions with different under cover resistance coefficient has been established. The effects of grain size on densimetric Froude number for incipient motion of bed material have been investigated. A relationship between the densimetric Froude number for incipient motion of bed material and the median grain size of bed material as well as the roughness coefficient of channel bed and roughness coefficient of ice cover has been established.

Key words: densimetric Froude number, grain size, ice cover, incipient motion, resistance coefficient, shear Reynolds number, velocity

1. Introduction

River ice represents an important hydrologic element in temperate and polar environments. An ice cover alters the hydraulics of an open channel by imposing an extra boundary to the flow, altering the water level and flow velocity compared to the ice free conditions^[1]. Ice alters the flow regime and the transport of sediment by temporarily storing water through ice jams, and results in differences in riverbed deformation as compared to that observed under open

flow conditions^[1-5]. Figure 1 shows the impacts of ice cover on water levels at the Toudaoguai Gauging Station on the Yellow River^[6]. Generally speaking, when ice floes move discretely and freely (for example, in the case of low surface concentrations of ice pans during freeze-up), the ice resistance effect is minimal and water levels do not change significantly. However, the formation of a stable ice cover effectively doubles the wetted perimeter compared to open channel conditions, and the associated increase in resistance to flow results in a significant increase in water level for the same discharge. It can therefore be expected that changes in flow condition will influence sediment motion. This aspect needs investigation.

* Project supported by the National Natural Science Foundation of China (Grant No.10372028).

Biography: WANG Jun (1962-), Male, Ph. D., Professor

Corresponding author: SUI Jue-yi, E-mail: sui@unbc.ca

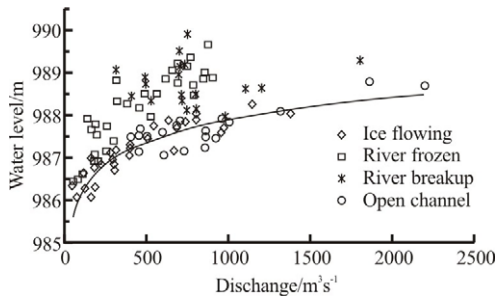


Fig.1 Rating curve of the Toudaoguai Gauging Station on the Yellow River in China

Studies have been conducted to understand the characteristics of sediment transport, including bedform development under ice covered conditions [7-11]. Hains and Zabilansky [12] have conducted experimental studies to investigate the local scour around bridge piers under ice covered conditions. Comparing with the scour process under open flow conditions, they investigated the variation in scour depth under different approach flow depth and mean velocity conditions. They found the scour depth under ice-covered conditions to be greater than that for open channel conditions with the difference being over 10% after 2 h of scouring, and increasing with the duration of scouring. This suggests that the increase in near-bed kinetic energy contributes to bed material transport under ice covered conditions than in the open channel flow case.

Consistent with data available for open channel conditions, it would be useful to understand the incipient movement of sediment under ice covered flow conditions. In the present study, a series of experiments have been carried out to investigate the effect of ice cover roughness and bed roughness on the velocity and Froude number for incipient motion of non-cohesive bed material, comparing to that under open flow conditions.

2. Experiments

Extensive clear-water experiments were conducted in a 18.0 m long, 0.50 m wide and 0.60 m deep recirculating flume, with glass walls and a concrete bottom (Fig.2). Two pumps delivered water from a 100 m³ underground sump to a 12 m³ head-tank, providing a maximum flow of 150 L/s, with inflow measured using a V-notch weir. An adjustable tailgate at the downstream end of the flume was used to control the water level and hence the flow velocity in the flume.

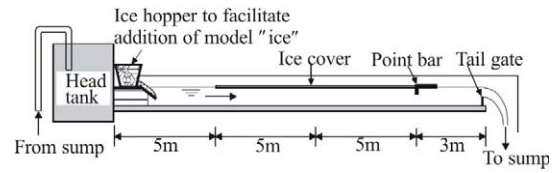


Fig.2 Schematic layout of experimental apparatus

The sheet ice cover was simulated using a floating foam panel, held in place by point bars installed on the flume wall. The measurement station was 10 m downstream of the head tank and the velocity profiles were measured at the channel centerline. To investigate the impacts of various degrees of under ice resistance on flow velocity and Froude number for incipient motion of bed material, untreated foam panels (simulated ice cover) were used as the smooth ice cover. The foam panels were modified by adding small wood pieces to create rough underside surfaces.

Velocities were measured using both a velocity-stage meter (SLY-89A) and a photoelectrical velocity meter (MZL-A). The velocity-stage meter was interfaced to a computer with measured flow velocity shown directly on the monitor. The photoelectrical velocity meter (MZL-A) was connected to a data logger. Both velocity meters were calibrated by the manufacturer (Nanjing Institute of Automation in Water Resources and Hydrology, China), who determined the instrument error to be less than about 0.5%. Additionally, at each measurement point flow velocities were measured thrice over a sampling duration of 5 min, with the average of these three values taken as representative of the actual flow velocity for that point.

Prior to conducting each experiment, the sand bed in the flume was leveled. Three types of non-cohesive sand with median grain size of $d_{50} = 0.32$ mm, 0.85 mm and 1.32 mm were used, respectively. The associated geometric standard deviations ($\sigma_g = (D_{84}/D_{16})^{0.5}$) were 1.73 for $d_{50} = 0.32$ mm, 1.28 for the $d_{50} = 0.85$ mm case, and 1.43 for $d_{50} = 1.32$ mm case.

To determine the composite Manning resistance coefficient for the cross section, the following one-dimensional equation for steady flow was applied.

$$\frac{\partial H}{\partial x} + \frac{1}{2g} \frac{\partial}{\partial x} \left(\frac{Q^2}{A^2} \right) + \frac{n^2 Q^2}{B^2 h^{10/3}} = 0 \quad (1)$$

The equation can be written in a difference form as:

Table 1 Manning resistance coefficient of ice cover and channel bed under various experimental conditions

Number of runs	Range of water depth (mm)	d_{50} (mm) of bed material	Types of ice cover	Under ice resistance (n_i)	Bed roughness (n_b)
33	66.6- 266.6	0.850	Smooth	0.0212	0.0128
28	66.8- 230.5	1.320	Smooth	0.0212	0.0139
25	78.0- 290.6	0.850	Rough	0.0347	0.0128
30	69.4 - 236.0	1.320	Rough	0.0347	0.0139

$$H_1 = H_2 + \Delta x \frac{n^2 Q^2}{B^2 \bar{h}^{10/3}} + \frac{Q^2}{2g} \cdot \left(\frac{1}{B_2^2 h_2^2} - \frac{1}{B_1^2 h_1^2} \right) \quad (2)$$

where, H is the water level (elevation), B is the channel widths, h is the water depth, n is the composite Manning's resistance coefficient for the section, and Q is the discharge. Subscripts 1 and 2 denote the entrance and exit cross sections, respectively. The overbar represents mean of variables. Based on the measured discharges and water levels, composite Manning resistance coefficients were calculated for each test run using Eq. (2). Based on this computed composite resistance, along with a reasonable approximation of the bed resistance coefficient (e.g. based on the values determined for comparable open water conditions) Sabeneev's equation^[13] can be used to deduce approximate values of the under ice roughness. Table 1 presents the results of this analysis.

3. Impacts of resistance coefficient on the location of maximim velocity

Threshold entrainment of a particle occurs when the drag force of a moving fluid acting on an exposed particle exceeds the weight force of gravity acting to hold that particle in place^[14]. The primary factors controlling threshold entrainment are flow velocity, streambed particle size, particle density, particle surface area exposed to the flow, and the pivoting angles among particles. In open channel flow, with increase in distance from riverbed, flow velocity

typically increases with the reduced influences of the shear stress of the channel bed on the fluid. Thus, flow velocity has a smaller value near channel bed, and typically reaches a maximum value near the water surface. In narrow channels, or near the banks in wide channels, the maximum velocity in the vertical profile will not occur at the surface but instead it will be located slightly below, due to the influences of the side banks.

An imposed ice cover results in an increased composite resistance, and thus, leads to a decrease in mean flow velocity. Under ice covered conditions, the flow in the upper portion of the flow is primarily affected by the ice cover resistance, while the lower portion of the flow is primarily influenced by the river bed resistance. The maximum velocity is located between the ice cover and the riverbed, with its vertical location dependent on the relative magnitudes of the river bed and ice underside resistance coefficients^[14]. At the centre of a relatively wide and symmetric cross section, the maximum flow velocity will be located on the midpoint of the flow depth for the case where the resistance coefficient of the underside of the ice cover equals that of the river bed. In this case the locus of points of maximum velocity in the section provides a reasonable approximation of the location of the zero shear interface between the ice and bed affected portions of the flow. When the river bed and ice cover have different resistance coefficients, the point of maximum flow velocity will be situated closer to the surface (channel bed or ice cover) where the resistance coefficient is less. In this case, locus of points of maximum velocity in the section does not coincide with a zero shear interface, and there will in fact be momentum transfer between the upper and lower portions of the flow^[15]. In this case, the plane of zero shear stress will lie substantially closer the smoother boundary^[16].

In all cases for the experiments in this study, the bed resistance was less than that of the ice underside (Table 1). Consequently, the near-bed velocity under ice covered conditions was higher than that for the case of open channel flow. Figures 3(a) and 3(b) illustrate examples of centerline velocity profiles measured over the finer bed material used ($d_{50} = 0.85$ mm) for two different flow depths, illustrating the effect of increasing under ice resistance on the shape of the velocity profiles. Y is the distance from ice cover or water surface to the measured point, h is the total water depth, and V is the corresponding mean velocity at that point. Note that in all cases (for the incipient movement of sand material), the flow velocity immediately under the ice cover and at the channel bed could not be measured, and were assumed to be zero (i.e. no-slip condition).

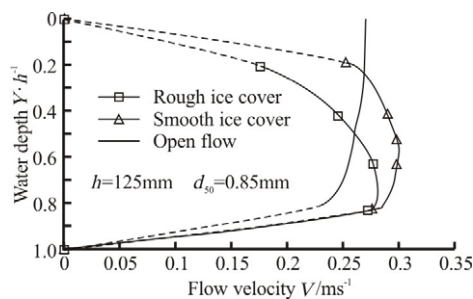


Fig.3(a) Incipient bed motion velocity profiles under ice cover with different resistance coefficient (total water depth $h = 125$ mm and $d_{50} = 0.85$ mm)

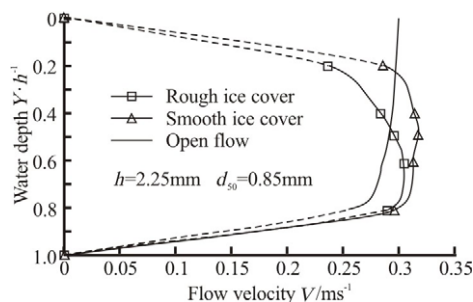


Fig.3(b) Incipient bed motion velocity profiles under ice cover with different resistance coefficient (total water depth $h = 225$ mm and $d_{50} = 0.85$ mm)

Therefore, for a given flow depth, even though the mean cross sectional flow velocity was less for the ice covered case than for the corresponding open channel flow, the near-bed velocity was higher. This increased gradient of near-bed velocity results in a higher shear stress on the bed for the ice covered case, thus it would be expected that the threshold velocity for initiation of sediment movement would decrease as ice cover resistance increases. Figure 4 confirms this tendency, illustrating the dependency of the ratio

of the location of the maximum velocity (Y_M from ice cover) to the total water depth (h) on the ratio of the resistance coefficient of ice cover (n_i) to the resistance coefficient of channel bed (n_b). As the ice resistance ratio (n_i/n_b) increases, the location of the maximum velocity moves closer to the channel bed.

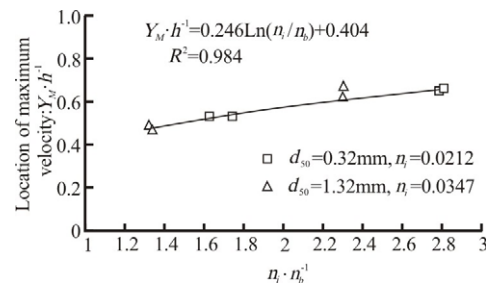


Fig.4 Dependence of the location of maximum velocity (water depth from ice cover) on the ratio of the resistance of ice cover to that of bed (n_i/n_b)

4. Hydraulic parameters for incipient motion of sand

4.1 Mean velocity for incipient motion of bed material

The velocity distribution under an ice cover can be considered as a quasi-logarithmic distribution [17-20]. Therefore, the flow velocity for incipient motion of bed material under ice should be different from that under open flow conditions.

For non-uniform bed material with median grain sizes of $d_{50} = 1.32$ mm, $d_{50} = 0.85$ mm, and $d_{50} = 0.32$ mm respectively, Figs. 5(a), 5(b) and 5(c) show the dependency of the mean flow velocity for incipient motion of bed material on the resistance of the ice cover and the flow depth. The following observations are noted:

(1) As shown in Figs. 3(a) and 3(b), for the same bed material (same median grain size), increasing ice resistance resulted in a lowering of the maximum velocity towards the channel bed. Thus, more kinetic energy will be contributed to bed material. As a result, for the same bed material, the flow velocity required for incipient motion of bed material under ice-covered conditions decreases with the increase in the resistance coefficient of ice cover. In the limiting case, flow velocity required for incipient motion of bed material for open flow is the highest.

(2) Provided the resistance coefficient of channel bed and ice cover doesn't change, for the same bed material (same median grain size), flow velocity required for the incipient motion of bed material increases with water depth.

(3) For a flow under an ice cover with the same resistance coefficient and flow depth, the large sized bed material clearly needs a higher flow velocity for incipient motion, as would be expected in Figs.5(a),

5(b) and 5(c).

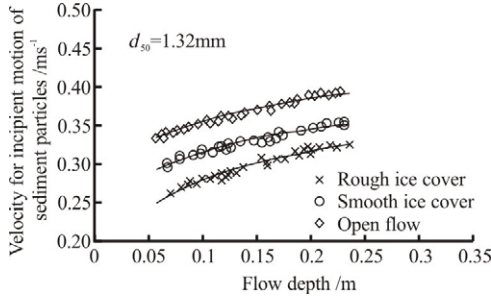


Fig.5(a) Relationship between the starting velocity of sediment and flow depth (non- uniform sediment with medium grain size of $d_{50} = 1.32\text{mm}$)

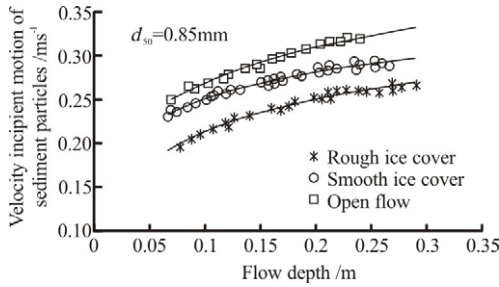


Fig.5(b) Relationship between the starting velocity of sediment and flow depth (non- uniform sediment with medium grain size of $d_{50} = 0.85\text{mm}$)

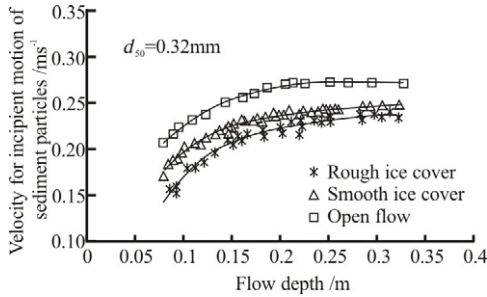


Fig.5(c) Relationship between the starting velocity of sediment and flow depth (non- uniform sediment with medium grain size of $d_{50} = 0.32\text{mm}$)

4.2 Dimensionless shear stress vs. shear Reynolds number for incipient motion

The incipient motion of particles must depend on, at least: boundary shear stress, sediment and fluid density (buoyancy), and grain size. In practice, the shear Reynolds number (Re^*) is usually used to study the incipient motion of particles.

$$Re^* = \frac{U_* D}{\nu} \quad (3)$$

where, U_* is the shear velocity, D is the grain size diameter, ν is the kinetic viscosity of fluid, g is the gravitational acceleration. For uniform or near-uniform flow, the frictional shear velocity is given as:

$$U_* = \sqrt{gRS} \quad (4)$$

where, S is the hydraulic slope, and R is the hydraulic radius. However, for this particular experimental study under ice covered condition, since the bed materials used are non-uniform natural sediment, the particle grain size varies. Therefore, the rigorous shear Reynolds number cannot be determined by using D for uniform sand. Thus, we used d_{50} to represent the particle size D and discuss the incipient motion of bed material under ice cover.

The Shields criterion indicates that the stability of a particle is dependent upon the applied stress (shear velocity), submerged weight of the particle, and shear Reynolds number. For this particular experimental study under ice covered condition, the Shields criterion (or dimensionless shear stress) is expressed as,

$$\tau_* = \frac{\rho U_*^2}{(\rho_s - \rho) g d_{50}} \quad (5)$$

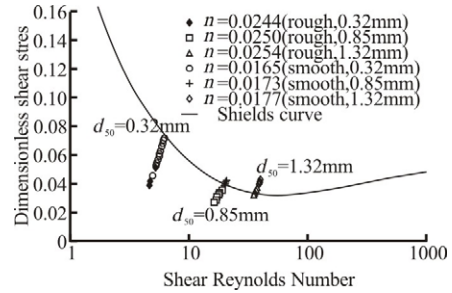


Fig.6 Dimensionless shear stress (τ_*) vs. shear Reynolds number (Re^*) for incipient motion of sediment

where, ρ and ρ_s are the mass density of water and sediment, respectively. As shown in Fig.6, the relation between the shear Reynolds number and dimensionless shear stress for the incipient motion of sediment under ice covered condition have been established for these three types of sediments with median grain sizes of $d_{50} = 1.32\text{mm}$, $d_{50} = 0.85\text{mm}$ and $d_{50} = 0.32\text{mm}$, respectively. From Fig.6, the following observations are noted.

(1) Overall, for bed material of same grain size, the larger the shear Reynolds number, the greater the

dimensionless shear stress for incipient motion of bed material. For the same dimensionless shear stress, the finer the particle, the lower the shear Reynolds number for the incipient motion of sediment. Under the same under cover resistance coefficient (n_i), the coarser the bed material, the greater the shear Reynolds number for the incipient motion of bed material under ice cover.

(2) For the same bed material (same d_{50}), and namely, the same resistance coefficient of channel bed, the resistance coefficient of ice cover plays an important role on the incipient motion of bed material. Results indicate that the dimensionless shear stress for incipient motion of sediment increases with the shear Reynolds number as the ice cover becomes rougher.

(3) For finer particles, such as $d_{50} = 0.32\text{mm}$ and $d_{50} = 0.85\text{mm}$, the critical dimensionless shear stress for incipient motion of bed material lies below the Shields curve for incipient motion of bed material under open flow condition. However, the critical dimensionless shear stress for incipient motion of coarser sand, $d_{50} = 1.32\text{mm}$, falls on the Shields curve for incipient motion of bed material under open flow condition.

4.3 Relationship between Froude number for incipient motion of bed material and associated parameters

As discussed above, the incipient motion of bed material depends not only on the hydraulic variables under ice-covered condition, but also on the properties of bed material. Additionally, the boundary conditions of cross section also play an important role on the incipient motion of bed material. Thus, densimetric Froude number of flow ($F_o = v_i / \sqrt{g d_{50} (\rho_s - \rho) / \rho}$) is an important variable used to describe hydraulic condition and bed material. Although the Shields parameter can be used to assess the incipient motion of bed material, F_o is more practical to be used. In this experimental study, the densimetric Froude number was determined using the mean flow velocity and mean grain size of bed material.

To quantitatively describe the dependence of the densimetric Froude number for incipient motion of bed material on the associated variables, both the boundary conditions and features of bed material should be considered. On the basis of a series of experiments, a relationship between the densimetric Froude number for incipient motion of bed material and the median grain size of bed material (d_{50}), mass density of bed material (ρ_s) and water (ρ) as well as the roughness coefficient of both channel bed (n_b) and ice cover (n_i) has been established as shown in Fig.7 and the following equation:

$$\frac{v_i}{\sqrt{\frac{g d_{50} (\rho_s - \rho)}{\rho}}} = 2.605 \ln(X) + 9.173 (R^2 = 0.983)$$

with

$$X = \left(\frac{d_{50}}{h}\right)^{-0.178} n_i^{-0.193} n_b^{0.989} \quad (6)$$

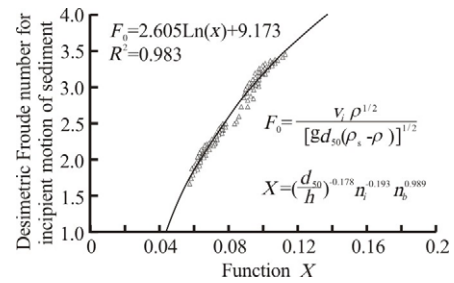


Fig.7 Dependence of densimetric Froude number for incipient motion of bed material on associated parameters

From Fig.7 and Eq.(6), following outcomes are summarized:

(1) For the same bed material (d_{50}/h), the more the roughness coefficient of ice cover (n_i), the less the densimetric Froude number for incipient motion of bed material, since a larger roughness coefficient of ice cover leads to an increased near-bed velocity. And thus, it can move larger particles.

(2) In contrast, for the same bed material (d_{50}/h), the more the roughness coefficient of channel bed (n_b), the more the densimetric Froude number for incipient motion of bed material, since a larger roughness coefficient of river bed leads to a decreased near-bed velocity. And thus, it can only move smaller particles.

(3) For the same boundary conditions (n_i and n_b), the larger the particle (d_{50}/h) more the densimetric Froude number for incipient motion of bed material, since a larger particles require more kinetic energy to move them.

5. Conclusion

Based on a series of experiments under both ice-covered and open flow conditions, the present

article discusses the flow velocity and water depth under ice cover for incipient motion of bed material. It is found that the deeper the flow depth under ice cover, the higher the flow velocity needed for the incipient motion of bed material. With the increase in the ratio of under cover resistance coefficient to the resistant coefficient of channel bed (n_i/n_b), the location of the maximum velocity moves to the bed. It is found that the water depth from ice cover to the location of the maximum velocity increases linearly with the resistance coefficient ratio (n_i/n_b). Results show that, for the same flow depth, the near-bed velocity under ice cover is clearly higher than that in open channel flow. And thus, the mean flow velocity for incipient motion of bed material under ice-covered conditions decreases with the increase in the resistance coefficient of ice cover. The diagram describing the dependence of the dimensionless shear stress for the incipient motion of sediment on the shear Reynolds number and resistance coefficient of ice cover has been established. The larger the shear Reynolds number, the greater the dimensionless shear stress for incipient motion of bed material. For the same dimensionless shear stress, the finer the particle, the lower the shear Reynolds number for the incipient motion of sediment. Under the same under cover resistance coefficient, the coarser the bed material, the greater the shear Reynolds number for the incipient motion of bed material under ice cover. For the same bed material, the dimensionless shear stress for incipient motion of sediment increases with the shear Reynolds number as the ice cover becomes rougher. For finer particles, such as $d_{50} = 0.32\text{mm}$ and $d_{50} = 0.85\text{mm}$, the critical dimensionless shear stress for incipient motion of bed material lies below the Shields curve for incipient motion of bed material under open flow condition. However, the critical dimensionless shear stress for incipient motion of coarser sand, $d_{50} = 1.32\text{mm}$, falls on the Shields curve for incipient motion of bed material under open flow condition. For the same bed material (d_{50}/h), the more the roughness coefficient of ice cover (n_i), the less the densimetric Froude number for incipient motion of bed material, since a larger roughness coefficient of ice cover leads to an increased near-bed velocity. And thus, it can move larger particles. In contrast, for the same bed material (d_{50}/h), the more the roughness coefficient of channel bed (n_b), the more the densimetric Froude number for incipient motion of bed material, since a larger roughness coefficient of river bed leads to a decreased near-bed velocity. For the same boundary conditions (n_i and n_b), the larger the particle (d_{50}/h) more the densimetric Froude number for incipient motion of bed material.

Acknowledgement

We would like to acknowledge the comments on the manuscript made by Dr. Hicks F. of the University of Alberta.

REFERENCES

- [1] SHEN H. T., WANG D. Under cover transport and accumulation of frazil granules[J]. **Journal of Hydraulic Engineering, ASCE**, 1995, 121(2) :184-195.
- [2] SUI J., WANG D. and KARNEY W. B. Sediment concentration and deformation of riverbed in a frazil jammed river reach[J]. **Canadian Journal of Civil Engineering**, 2000, 27 (6):1120-1129.
- [3] SUI J., KARNEY W. B. and SUN Z. et al. Field investigation of frazil jam evolution – a case study [J]. **Journal of Hydraulic Engineering, ASCE**, 2002, 128 (8):781-787.
- [4] SUI J., KARNEY W. B. and WANG J. Coarsening of sediment concentration under ice-covered condition[C]. **Proceedings of the 9th International Conference on River Sediment**. Yichang, China, 2004, 3:1388-1394.
- [5] SUI J., JACKSON P. and FANG D. J. **Investigations of the sediment budget of a reach of the Yellow River in the Loess Plateau**[M]. Wallingford, Oxfordshire, UK: IAHS Press, 2005, 172-181.
- [6] SUI J., THRING R. and KARNEY W. B. et al. Effects of river ice on stage-discharge relationship- a case study of the Yellow River[J]. **International Journal of Sediment Research**, 2007, 22(4): 263-272.
- [7] SAYRE W. W., SONG G. B. Effects of ice covers on alluvial channel flow and sediment transport processes[R]. IIHR Report No. 218, University of Iowa, 1979.
- [8] LAU Y. L. and KRISHNAPPAN B. G. Sediment transport under ice cover[J]. **Journal of Hydraulic Engineering, ASCE**, 1985, 111 (6): 934-950.
- [9] SMITH B. T., ETTEMA R. Ice-cover influence on flow and bedload transport in dune-bed channels[R]. IIHR Report No. 374, University of Iowa, 1995.
- [10] TSAI W. F., ETTEMA R. Ice cover influence on transverse bed slopes in a curved alluvial channel[J]. **Journal of Hydraulic Research**, 1994, 32(4):561-581.
- [11] ETTEMA R., BRAILEANU F. and MUSTE M. Method for estimating sediment transport in ice covered channels[J]. **Journal of Cold Region Engineering, ASCE**, 2000, 14:130-144.
- [12] HANIS D., ZABILANSKY L. Laboratory test of scour under ice: data and preliminary results[R]. US Army CREEL Research Report, tr-04-09, 2004, 77-118.
- [13] ASHTON G. D. **Lake and river ice engineering**[M]. Littleton, CO:Water Resources Publications, 1986.
- [14] LORANG M., HAUER R. Flow competence and streambed stability: an evaluation of technique and application[J]. **Journal of the North American Benthological Society**, 2003, 22(4):475-491.
- [15] HANIALIC K., LAUNDER B. E. Fully developed asymmetric flow in a plane channel[J]. **Journal of Fluid Mechanics**, 1972, 51:301-335.

- [16] GOGUS M., TATINCLAUX J. C. Mean characteristics of asymmetric flows, application to flow below ice jams[J]. **Canadian Journal of Civil Engineering**, 1981, 8(3):342-350.
- [17] CHEES. P., RAY S. Multiple resistance ice covered channels[C]. **Proceedings of the International Symposium on Ice**. Iowa, USA, 1986, 53-62.
- [18] SMITH B. A laboratory study of flow in ice covered dune bed channels[C]. **Proceedings of the International Symposium on Ice**. Banff, Canada ,1992, 1323-1332.
- [19] YAMASHITA S., SHIMIZU Y. Characteristics of shear stress in the ice covered river[C]. **Proceedings of the International Symposium on Ice**. Banff, Canada ,1992, 356-360.
- [20] DOLGOPOLOVA E. N. Resistance of ice covered nature flows[J]. **Proceedings of the International Symposium on Ice**. Beijing, China, 1996, 497-504.